of $(NH_4)_2S_5$ solutions depend on the excitation line; this was not the case for Li_2S_5 solutions.

IV. Determination of the Extinction Coefficient of S_4^{2-}. The determination of the extinction coefficient of S_4^{2-} is based on the following assumptions: (i) The disproportionation of S_4^{2-} for the dilute $(NH_4)_2S_n$ solutions studied with UV-visible spectrophotometry can be written

$$2S_4^{2-} \rightleftarrows 2S_3^- + S_2^{2-} \quad (22)$$

(ii) The absorbance at 390 nm, $A(390)$ is due to S_4^{2-}. (iii) The concentration C_0 of S_4^{2-} at 200 K is equal to the overall concentration of the $(NH_4)_2S_4$ solution. The absorbance $A(390)$ and $A(610)$ are then related by

$$A(390) = -\frac{\epsilon(S_4^{2-})}{\epsilon(S_3^-)}A(610) + C_0 d[\epsilon(S_4^{2-})] \quad (23)$$

where d is the optical path length. The experimentally measured absorbances $A(390)$ and $A(610)$ are found to be linearly related, when the measured absorbances are corrected for the thermal variations of the density of the solution. For all the $(NH_4)_2S_4$ solutions investigated, it was found that $\epsilon(S_4^{2-}) = 1300 \pm 150$ M^{-1} cm^{-1} and that $\epsilon(S_3^-) = 4600 \pm 400$ M^{-1} cm^{-1}. This value obtained for $\epsilon(S_3^-)$ is quite compatible with that found in Li_2S_6 or $(NH_4)_2S_6$ solutions. The value obtained for $\epsilon(S_4^{2-})$ has to be compared with the value $\epsilon(S_4^{2-}) = 900$ M^{-1} cm^{-1} given by Martin et al. in DMSO solutions.[12]

A similar analysis was done in Li_2S_4 solutions[4] and gave $\epsilon(S_4^{2-}) = 1100$ M^{-1} cm^{-1} but $\epsilon(S_3^-) \simeq 2000$ M^{-1} cm^{-1}. This suggests that the analysis based on eq 22 and 23 is more realistic in $(NH_4)_2S_4$ solutions; the disproportionation is larger in ammonium solutions, and eq 22 gives more precise results.

Acknowledgment. We are grateful to the Laboratoire de Spectroscopie Infrarouge et Raman (LASIR) de l'Université de Lille 1, Lille, France, for the use of their Raman spectrometers. We thank Drs. Lorriaux, Chapput, and de Bettignies for experimental assistance and Dr. Corset for helpful discussions. This research was supported by the CNRS (ATP Application de l'électricité à la chimie No. 249) and by the AFME (décision d'aide à la Recherche No. 4 213 9261). We also thank Dr. F. X. Sauvage for a critical reading of the manuscript.

Registry No. S, 7704-34-9; NH_3, 7664-41-7; H_2S, 7783-06-4; N_2H_4·HCl, 2644-70-4; $(NH_4)_2S_2$, 113894-22-7; $(NH_4)_2S_4$, 74238-82-7; $(NH_4)_2S_5$, 12135-77-2; $(NH_4)_2S_6$, 113894-04-5; S_3^-, 12597-04-5; S_4^-, 12597-07-8; $(NH_4)_2S_{10}$, 110299-90-6; $(NH_4)_2S_8$, 83682-24-0.

Contribution from the Department of Chemistry, University of South Carolina, Columbia, South Carolina 29208

Synthesis, X-ray Crystal Structure, and Multinuclear NMR Study of the Dynamic Behavior of Tris[dihydrobis(1-pyrazolyl)borato]yttrium(III): A Molecule with Three Three-Center, Two-Electron Bonds

Daniel L. Reger,* Jeffrey A. Lindeman, and Lukasz Lebioda

Received February 17, 1988

Reaction of YCl_3 with $K[H_2B(pz)_2]$ (pz = pyrazolyl ring) and $K[H_2B(3,5\text{-}Me_2pz)_2]$ yields $[H(\mu\text{-}H)B(pz)_2]_3Y$ (**1**) and $[H(\mu\text{-}H)B(3,5\text{-}Me_2pz)_2]_3Y$ (**2**). The molecular structure of **1** has been determined by single-crystal X-ray diffraction: monoclinic, space group $P2_1/n$, $a = 14.231$ (3) Å, $b = 22.959$ (4) Å, $c = 9.342$ (2) Å, $\beta = 104.06$ (2)°, $V = 2961$ Å^3, and $Z = 4$. The six nitrogen donor atoms are arranged in a nearly perfect trigonal prism. Each of the three rectangular faces of the trigonal prism is capped by a three-center B-H···Y agostic bond. The observation of B-H stretching bands at low frequencies in the solution IR spectra and the nonequivalence of the BH_2 hydrogen atoms in low-temperature NMR spectra demonstrates these agostic bonds are maintained in solution. Low-temperature ^{13}C NMR spectroscopy shows that the pyrazolyl rings are also nonequivalent, forming a 1/1 set. Thus, the solution structure is different from that of the solid by a twisting of the triangular faces of the trigonal prism toward an octahedral geometry. The molecules are fluxional in solution, both the pyrazolyl rings and BH_2 hydrogen atoms becoming equivalent in ambient-temperature spectra. The barriers to equilibration of the pyrazolyl rings and the BH_2 hydrogen atoms are the same (11.4 kcal/mol from the carbon data), indicating a common dynamic process. This process is proposed to be breaking of the agostic bonds and flipping of the boat arrangement of the six-membered BN_4Y rings, with re-formation of the bridging interactions on the adjacent faces. A common mechanism involving breakage of the agostic interaction is supported by a small isotope effect in the equilibration of the pyrazolyl rings measured in the barrier of **1** and its isotopomer $[D(\mu\text{-}D)B(pz)_2]_3Y$. Compound **2** shows similar fluxional behavior in solution with a measured barrier of 11.8 kcal/mol. Resonances in the ^{89}Y NMR spectra at 238.8 ppm for **1** and 105.6 ppm for **2** are observed. These data are best collected by using the INEPT pulsing sequence.

Introduction

We have been exploring the chemistry of polypyrazolylborate complexes of the early transition metals.[1,2] Part of our plan in using this flexible ligand system is to prepare complexes by using the trischelating $[RB(pz)_3]^-$ ligand (pz = pyrazolyl ring) as a six-electron donor and to also prepare similar complexes with the four-electron-donor bischelating $[R_2B(pz)_2]^-$ ligands. If successful, the second series would have potentially two fewer electrons donated to the metal, and this could drastically alter reaction chemistry. We have prepared two sets of complexes of this type. In both sets, $[HB(3,5\text{-}Me_2pz)_3]TaMe_3Cl/[H(\mu\text{-}H)B(3,5\text{-}Me_2pz)_2]TaMe_3Cl$[1] and $[HB(pz)_3]CpZrCl_2/[H(\mu\text{-}H)B(pz)_2]\text{-}CpZrCl_2$,[2d] the complex prepared with the $[H_2B(pz)_2]^-$ ligand shows an interesting three-center, two-electron B-H···metal interaction making the ligand a six-electron donor to the metal. This type of agostic interaction[3] has also been observed with molybdenum-polypyrazolylborate complexes[4] and very recently with ruthenium complexes.[5]

We have recently expanded our study to the chemistry of yttrium.[6] With zirconium and tantalum, we were unable to

(1) (a) Reger, D. L.; Swift, C. A.; Lebioda, L. *Inorg. Chem.* **1984**, *23*, 349. (b) Reger, D. L.; Swift, C. A.; Lebioda, L. *J. Am. Chem. Soc.* **1983**, *105*, 5343.
(2) (a) Reger, D. L.; Tarquini, M. E. *Inorg. Chem.* **1982**, *21*, 840. (b) Reger, D. L.; Tarquini, M. E. *Inorg. Chem.* **1983**, *22*, 1064. (c) Reger, D. L.; Tarquini, M. E.; Lebioda, L. *Organometallics* **1983**, *2*, 1763. (d) Reger, D. L.; Mahtab, R.; Baxter, J. C.; Lebioda, L. *Inorg. Chem.* **1986**, *25*, 2045.
(3) Brookhart, M.; Green, M. *J. Organomet. Chem.* **1983**, *250*, 395.
(4) (a) Kosky, C. A.; Ganis, P.; Avitabile, G. *Acta Crystallogr., Sect. B: Struct. Crystallgr. Cryst. Chem.* **1971**, *B27*, 1859. (b) Cotton, F. A.; Jeremic, M.; Shaver, A. *Inorg. Chim. Acta* **1972**, *6*, 543.
(5) Albers, M. O.; Crosby, S. F. A.; Liles, D. C.; Robinson, D. J.; Shaver, A.; Singleton, E. *Organometallics* **1987**, *6*, 2014.
(6) Reger, D. L.; Lindeman, J. A.; Lebioda, L. *Inorg. Chim. Acta* **1987**, *139*, 71.

0020-1669/88/1327-1890$01.50/0

prepare complexes containing two polypyrazolylborate ligands. The larger size of yttrium should allow for the coordination of more than one polypyrazolylborate ligand. In fact, Takats has prepared[7] a series of complexes of the formula $[HB(pz)_3]_3M$ (M = Y, La, Ce, Pr, Sm, Gd, Er, Yb, Lu) and has carefully characterized the ytterbium complex as eight-coordinate $[\eta^3\text{-}HB(pz)_3]_2[\eta^2\text{-}HB(pz)_3]Yb$ in both the solid[8] and solution[9] phases. One specific goal of our program was the synthesis of $[H_2B(pz)_2]_3Y$. We anticipated that this complex could have multiple agostic B-H···Y interactions. Reported here is the synthesis, solid-state characterization by X-ray crystallography, and multinuclear (^1H, ^2H, ^{13}C, ^{11}B, ^{89}Y) variable-temperature NMR study of this complex. The synthesis and study of $[H_2B(3,5\text{-}Me_2pz)_2]_3Y$ is also reported. These complexes contain three three-center, two-electron bonds in both the solid and solution phases and are fluxional in solution.

Experimental Section

General Procedure. All operations are carried out under a nitrogen atmosphere either with standard Schlenk techniques or in a Vacuum Atmospheres HE-493 drybox. All solvents were dried, degassed, and distilled prior to use. Infrared spectra were recorded on a Perkin-Elmer 781 spectrometer. The ^1H, ^2H, ^{11}B, and ^{13}C solution NMR spectra were recorded on a Bruker AM-300 spectrometer using a 5-mm broad-band probe. An IBM NR-80 spectrometer was also used to collect ^{13}C NMR data. Proton and deuterium chemical shifts are reported in ppm vs Me_4Si. ^{13}C chemical shifts are likewise reported vs TMS with the solvents CD_2Cl_2 and $CDCl_3$ as internal standards (CD_2Cl_2 resonance at 53.85 ppm, $CDCl_3$ at 77.00 ppm) for the solution spectra. Boron-11 chemical shifts are reported in ppm vs $BF_3{\cdot}OEt_2$. Solid-state ^{13}C MAS spectra were recorded on a Varian XL-300 spectrometer. Variable-temperature NMR analysis was also performed on the Bruker AM-300 NMR spectrometer at the following resonant frequencies: ^1H, 300.13 MHz; ^2H, 46.07 MHz; ^{11}B, 96.29 MHz; ^{13}C, 75.47 MHz. The samples for variable-temperature studies were dissolved in CD_2Cl_2 or $C_6D_5CD_3$, and then the solutions were sealed in screw-capped 5-mm NMR tubes. Activation parameters were calculated at the coalescence temperature.[10] Accurate mass spectra were run as solids on a VG 70SQ spectrometer, and low-resolution spectra, on a Finnigan 4521 GC–mass spectrometer. Clusters assigned to specific ions show appropriate isotopic patterns as calculated for the atoms present. Elemental analyses were performed by Robertson Laboratory, Inc. $K[H_2B(pz)_2]$ and $K[H_2B(3,5\text{-}Me_2pz)_2]$ were prepared by published methods.[11] $Na[D_2B(pz)_2]$ was prepared by substituting $NaBD_4$ for KBH_4 and by following the same procedure as for $K[H_2B(pz)_2]$. Anhydrous YCl_3 was purchased from Cerac/Pure Division and was used without further purification.

^{89}Y NMR Spectra. ^{89}Y NMR experiments were performed by using a Bruker AM-300 spectrometer equipped with a broad-band 10-mm probe at a resonant frequency of 14.71 MHz. Pulse widths were determined on a 1.0 M sample of YCl_3 in D_2O with a 90° pulse of 31.0 μs and a 180° pulse of 62.8 μs. Chemical shifts are reported in ppm versus the same 1.0 M YCl_3 in D_2O standard. The sample concentration ranged from 0.29 to 0.35 M for $[H_2B(pz)_2]_3Y$ and was 0.14 M for $[H_2B(3,5\text{-}Me_2pz)_2]_3Y$ in either $CDCl_3$ or CD_2Cl_2. Typical direct-acquisition experiments utilized a 13° pulse (4.5 μs) and a relaxation delay of 0.01–0.001 s with total acquisition times of several hours. Proton magnetization transfer experiments were carried out by using a coupled INEPT sequence and a refocussed INEPT sequence.[12] The polarization transfer delay, $\tau = 1/4J$, was optimized with the latter sequence by varying the delay time over a range from 0.02 to 0.60 s, with maximum signal intensity resulting from a delay of 0.48 s. A refocusing delay of 0.025 s was used but was unoptimized. The relaxation delay in the polarization transfer experiments was 4.0 s; thus, for acquisition of the 64 scans yielding a very good signal to noise ratio, the total acquisition time was less than 6 min.

Tris[dihydrobis(1-pyrazolyl)borato]yttrium(III) $[[H(\mu\text{-}H)B(pz)_2]_3Y]$ (1). YCl_3 (1.25 g, 6.41 mmol) and $K[H_2B(pz)_2]$ (3.94 g, 21.2 mmol) were placed in a 250-mL round-bottomed flask. THF (130 mL) was added by syringe, and the solution was stirred overnight at room temperature. The solution was filtered and the solvent removed under vacuum. The filtrate residue was extracted with CH_2Cl_2 (150 mL), the solution filtered, and the CH_2Cl_2 evaporated under vacuum, yielding a white solid (3.01 g, 5.68 mmol; 89%). Recrystallization from a concentrated $CDCl_3$ solution gave clear crystals suitable for X-ray analysis. ^1H NMR spectrum (CD_2Cl_2, ambient temperature): 7.62, 6.74 ppm (6, 6; d, d; J = 1.84, 1.79 Hz; 3-H, 5-H (pz)); 6.10 ppm (6, t, J = 1.98 Hz, 4-H (pz)); 3.82 ppm (6, br, BH_2). ^1H NMR spectrum (CD_2Cl_2, −83 °C): 7.64, 6.72 ppm (6, 6; s, s; 3-H, 5-H (pz)); 6.15 ppm (6, s, 4-H (pz)); 3.91, 3.59 ppm (3, 3; s, s; BH_2). ^{13}C solution NMR spectrum ($CDCl_3$, ambient temperature, 20.13 MHz): 139.7, 135.0 ppm (d, d; J_{CY} = 1.5, 0.5 Hz; 3-C, 5-C (pz)); 104.5 ppm (d, J_{CY} = 0.8 Hz, 4-C (pz)). ^{13}C solution NMR spectrum (CD_2Cl_2, −83 °C, 75.469 MHz): 139.73, 139.58, 135.41, 135.35 ppm (s, s, s, s; 3-C, 5-C (pz)); 104.66, 104.61 ppm (s, s; 4-C (pz)). Solid-state ^{13}C MAS NMR spectrum: 139.4, 135.6 ppm (3-C, 5-C (pz)); 104.5 ppm (4-C (pz)). ^{11}B NMR spectrum ($CDCl_3$): −8.94 ppm (t, J_{BH} = 110 Hz, line narrowed). ^{89}Y NMR spectrum (CD_2Cl_2, ambient temperature): 238.8 ppm. ^{89}Y NMR spectrum (CD_2Cl_2, −83 °C): 246.0 ppm. IR spectrum (Nujol mull), cm^{-1}: 2465, 2460, 2445 (BH); 2340, 2310, 2255, 2225 (μ-BH). IR spectrum ($C_2H_2Cl_2$), cm^{-1}: 2460, 2450, 2410 (BH); 2340, 2310, 2255, 2225 (μ-BH). The mass spectrum shows the highest cluster, $M^+ - H$, at m/e 529. Anal. Calcd for $C_{18}H_{24}N_{12}B_3Y$: C, 40.81; H, 4.57. Found: C, 40.70; H, 4.35.

Tris[dihydrobis(3,5-dimethyl-1-pyrazolyl)borato]yttrium(III) $[[H(\mu\text{-}H)B(3,5\text{-}Me_2pz)_2]_3Y]$ (2). YCl_3 (0.20 g, 1.0 mmol) and $K[H_2B(3,5\text{-}Me_2pz)_2]$ (0.80 g, 3.3 mmol) were placed in a 50-mL round-bottomed flask. THF (25 mL) was added by syringe, and the solution was stirred at room temperature for 4 h. The solvent was then evaporated under vacuum. The residue was dissolved in benzene (25 mL), the solution filtered, and the benzene removed under vacuum, yielding a white solid (0.52 g, 0.74 mmol; 74%). ^1H NMR spectrum (CD_2Cl_2, ambient temperature): 5.07 ppm (6, s, 4-H (pz)); 3.79 ppm (6, br, BH_2); 2.32, 1.25 ppm (18, 18; s, s; 3-Me, 5-Me). ^1H NMR spectrum (CD_2Cl_2, −89 °C): 5.66 ppm (6, s, 4-H (pz)); 3.79, 3.66 ppm (3, 3; s, s; BH_2); 2.26, 1.15 ppm (18, 18; s, s; 3-Me, 5-Me). ^{13}C solution NMR spectrum (CD_2Cl_2, ambient temperature): 149.53, 142.93 ppm (d, s; J_{CY} = 1.46 Hz, 3-C, 5-C (pz)); 105.57 ppm (s, 4-C (pz)); 10.78, 9.34 ppm (s, s; 3-Me, 5-Me). ^{13}C solution NMR spectrum (CD_2Cl_2, −89 °C): 149.53, 143.32 ppm (d, s; J_{CY} = 1.46 Hz, 3-C, 5-C (pz)); 105.70, 105.59 ppm (s, s; 4-C (pz)); 11.14, 11.11, 9.59, 9.52 ppm (s, s, s, s; 3-Me, 5-Me). ^{11}B NMR spectrum ($CDCl_3$): −13.8 ppm (t, J_{BH} = 116 Hz, line narrowed). ^{89}Y NMR spectrum ($CDCl_3$): 105.6 ppm. IR spectrum (Nujol mull), cm^{-1}: 2450 (BH); 2325, 2330, 2262, 2220 (μ-BH). The accurate mass spectrum shows $M^+ - H$ and $M^+ - (3,5\text{-}Me_2pzH_2)$ clusters. m/e: calcd for $C_{30}H_{47}N_{12}{}^{11}B_3Y$ and $C_{25}H_{39}N_{10}{}^{11}B_3Y$, 697.3384 and 601.2697; found, 697.3406 and 601.2731.

Tris[dideuteriobis(1-pyrazolyl)borato]yttrium(III) $[[D(\mu\text{-}D)B(pz)_2]_3Y$ (1-d_6). $[D(\mu\text{-}D)B(pz)_2]_3Y$ was prepared in the same manner as $[H(\mu\text{-}H)B(pz)_2]_3Y$, substituting $NaD_2B(pz)_2$ for $KH_2B(pz)_2$. ^{13}C solution NMR spectrum, (CD_2Cl_2, ambient temperature): 140.40, 135.87 ppm (s, s; 3-C, 5-C (pz)); 105.26 ppm (s, 4-C (pz)). ^{13}C solution NMR spectrum (CD_2Cl_2, −83 °C): 139.67, 139.52, 135.33, 135.27 ppm (s, s, s, s; 3-C, 5-C (pz)); 104.63, 104.58 ppm (s, s; 4-C (pz)). ^2H NMR spectrum (CD_2Cl_2, ambient temperature): 4.28 ppm (s, BD_2). ^2H NMR spectrum (CD_2Cl_2, −62 °C): 4.28, 4.00 ppm (s, s; BD_2). IR spectrum (Nujol mull), cm^{-1}: 1848, 1832 (BD); 1675 (μ-BD). The mass spectrum shows the highest cluster, $M^+ - D$, at m/e 534.

Crystallographic Analysis. Clear crystals of $[H(\mu\text{-}H)B(pz)_2]_3Y{\cdot}CDCl_3$ were grown from a concentrated $CDCl_3$ solution. They were extremely difficult to mount because of decomposition at ambient temperature due to loss of the chloroform of crystallization. The data crystal was mounted at −20 °C in a sealed capillary, and the X-ray data were collected at −100 °C to prevent decomposition of the crystal in the X-ray beam. Diffraction measurements were made on a CAD-4 diffractometer. The unit cell was determined and refined from 25 general reflections. Crystal data, data collection parameters, and results of the analysis are listed in Table I. The data were collected in concentric shells; one-third of the 38–46° shell had to be discarded due to a malfunction of the low-temperature device. The structure was solved by the heavy-atom method. Data reduction was carried out by using SDP,[13] and refinement calculations were carried out by using SHELX 76.[14] There is a partial disorder of the lattice solvent molecule, $CDCl_3$. It was accounted for by intro-

(7) Bagnall, K. W.; Tempest, A. C.; Takats, J.; Masino, A. P. *Inorg. Nucl. Chem. Lett.* **1976**, *12*, 555.
(8) Stainer, M. V. R.; Takats, J. *Inorg. Chem.* **1982**, *21*, 4050.
(9) Stainer, M. V. R.; Takats, J. *J. Am. Chem. Soc.* **1983**, *105*, 410.
(10) Kegley, S. E.; Pinhas, A. R. *Problems and Solutions in Organometallic Chemistry*; University Science Books: Mill Valley, CA, 1986; pp 20–23.
(11) Trofimenko, S. *J. Am. Chem. Soc.* **1967**, *89*, 3170.
(12) Garber, A. R. "INEPT"; NMR spectroscopy Applications Note 6; IBM Instruments, Inc.: Danbury, CT, 1983.
(13) Frenz, B. A. "Enraf-Nonius Structure Determination Package"; Enraf-Nonius: Delft, The Netherlands, 1983.
(14) Sheldrick, G. M. "SHELX-76, A Program for Crystal Structure Determination"; Cambridge University Press: Cambridge, England, 1976.
(15) Walker, N.; Stuart, D. *Acta Crystallogr., Sect. A: Found Crystallogr.* **1983**, *A39*, 158.

Table I. Crystallographic Data for the Structural Analysis

formula	$C_{18}H_{24}B_3N_{12}Y \cdot CDCl_3$
cryst system	monoclinic
space group	$P2_1/n$
a, Å	14.231 (3)
b, Å	22.959 (4)
c, Å	9.342 (2)
β, deg	104.06 (2)
V, Å^3	2961
Z	4
cryst size, mm	0.4 × 0.3 × 0.2; irregular fragment of prism
monochromator	graphite
radiation	Mo Kα (λ = 0.71073 Å)
temp, °C	−100
2θ range, deg	$4 < 2\theta < 46$
no. of reflcns measd	3493
no. of data used after sym averaging	3186
linear abs coeff, cm^{-1}	22.8 cm^{-1}
abs cor	ref 15
transmission factor	
max	1.232
min	0.885
av	0.986
cryst decay cor	
av	1.018
max	1.039
R_{int}	0.034
R_F	0.049
R_{wF}	0.053

ducing one pair of chlorine atoms with partial occupancy. The hydrogen atoms were placed in calculated positions except those coordinated to yttrium, which were located in the difference Fourier map. Full-matrix least-squares refinements were carried out with $w = (\sigma^2(F) + 0.0004F^2)^{-1}$ for reflections with $I > 3\sigma(I)$. Table II shows the atomic positional parameters, and Table III, the bond distances and bond angles relevant to the yttrium coordination sphere. Table IV (see supplementary material) shows bond distances and angles for the ligands.

Results and Discussion

Synthesis and Ambient-Temperature Characterization of Complexes. The complexes $[H(\mu\text{-}H)B(pz)_2]_3Y$ (**1**) and $[H(\mu\text{-}H)B(3,5\text{-}Me_2pz)_2]_3Y$ (**2**) (pz = pyrazolyl ring) are prepared as shown in eq 1. Both complexes are reasonably stable in air as solids

$$YCl_3 + 3K[H_2B(pz)_2] \rightarrow [H(\mu\text{-}H)B(pz)_2]_3Y + 3KCl \quad (1)$$

and only slowly decompose in solution. They are soluble in THF, halocarbons, and aromatic hydrocarbons and insoluble in saturated hydrocarbons. Both react with acetone to form a product that contains isopropyl groups, but we have not yet been able to definitively characterize these complexes.

The IR spectrum of complex **1** shows two complex B–H stretching bands centered at ca. 2455 and 2280 cm^{-1} in both the solution and solid state. Complex **2** also displays these bands centered at ca. 2450 and 2280 cm^{-1}. The higher frequency band can be clearly assigned to a normal terminal B–H stretch, while the lower band is assigned to a bridging B–H···Y interaction.[1,2] Although clearly the lowering of the B–H stretch is indicative of an interaction with the yttrium atom, the shift is relatively small, indicating that the bridging interaction is significantly weaker in the case of **1** and **2** than in the other known cases of molecules with this type of agostic interaction. For comparison, the B–H···M stretch in $[H(\mu\text{-}H)B(3,5\text{-}Me_2pz)_2]TaMe_3Cl$ (**3**) and $[H(\mu\text{-}H)B(pz)_2]CpZrCl_2$ (**4**) is observed at 2050[1b] and 2160[2d] cm^{-1}, respectively.

In our earlier work, it was shown that proton-coupled ^{11}B NMR spectroscopy was a definitive test for the presence of an agostic B–H···M bond. For both **3** and **4**, the ^{11}B spectra show a doublet of doublets with J_{BH} = ca. 118 and 80 Hz. The larger value is typical of a terminal B–H group whereas the smaller value is typical for a B–H···M group.[1a,2d] However, this method did not prove useful for the detection of a three-center interaction with **1** and **2**. The coupled ^{11}B NMR spectrum of **1** shows a triplet with J_{BH} = 110 Hz, and for that of **2** a triplet with J_{BH} = 116 Hz is observed. These results could indicate that **1** and **2** do not contain an agostic interaction (in conflict with the IR data) or be evidence for molecules with agostic interactions that equilibrate the boron hydrogen atoms by a dynamic process in solution. This type of dynamic process has not been observed previously for the known cases of polypyrazolylborate complexes with a B–H···M interaction.[1a,2d,4,5]

Table II. Fractional Atomic Coordinates (Esd's in Parentheses) and Equivalent Isotropic Temperature Factors

	x/a	y/b	z/c	B, Å^2
Y(1)	0.2694 (1)	0.1012 (0)	0.1207 (1)	2.32
Cl(1)	0.8311 (2)	0.1922 (1)	0.5354 (3)	7.18
Cl(2)	0.9447 (5)	0.2310 (3)	0.3357 (1)	12.42
Cl(3)	0.8098 (4)	0.1391 (2)	0.2581 (5)	13.82
Cl(2A)	0.9744 (7)	0.1521 (8)	0.4116 (16)	14.57
C(1)	0.8488 (9)	0.1996 (5)	0.3595 (13)	7.80
N(11)	0.4982 (5)	0.1194 (3)	0.2604 (7)	3.01
N(12)	0.4198 (5)	0.0973 (3)	0.3032 (7)	2.97
N(21)	0.4581 (4)	0.0961 (3)	−0.0111 (7)	2.74
N(22)	0.3717 (4)	0.0683 (3)	−0.0322 (7)	2.62
N(31)	0.2108 (5)	−0.0020 (3)	0.3165 (7)	2.83
N(32)	0.2122 (5)	0.0578 (3)	0.3160 (7)	2.74
N(41)	0.1644 (4)	−0.0223 (3)	0.0445 (7)	2.47
N(42)	0.1579 (4)	0.0322 (3)	−0.0148 (7)	2.44
N(51)	0.1656 (5)	0.2203 (3)	0.1847 (7)	3.18
N(52)	0.2501 (5)	0.1909 (3)	0.2413 (7)	2.82
N(61)	0.1262 (5)	0.1929 (3)	−0.0869 (8)	3.20
N(62)	0.2050 (5)	0.1596 (3)	−0.0919 (7)	2.73
C(13)	0.4521 (6)	0.0785 (4)	0.4389 (9)	3.37
C(14)	0.5500 (7)	0.0882 (4)	0.4900 (10)	4.52
C(15)	0.5760 (6)	0.1148 (4)	0.3747 (10)	4.25
C(23)	0.3696 (6)	0.0279 (4)	−0.1382 (9)	3.06
C(24)	0.4537 (7)	0.0306 (4)	−0.1843 (9)	3.29
C(25)	0.5079 (6)	0.0731 (4)	−0.1023 (9)	3.11
C(33)	0.1820 (6)	0.0745 (4)	0.4351 (10)	3.78
C(34)	0.1602 (7)	0.0268 (5)	0.5109 (9)	4.53
C(35)	0.1806 (7)	−0.0207 (4)	0.4301 (11)	4.54
C(43)	0.0836 (6)	0.0308 (4)	−0.1363 (9)	3.02
C(44)	0.0435 (6)	−0.0244 (4)	−0.1553 (9)	3.32
C(45)	0.0952 (6)	−0.0570 (4)	−0.0381 (9)	3.35
C(53)	0.3015 (6)	0.2248 (4)	0.3467 (9)	3.34
C(54)	0.2516 (7)	0.2759 (4)	0.3580 (10)	4.38
C(55)	0.1673 (7)	0.2710 (4)	0.2517 (10)	4.21
C(63)	0.2199 (6)	0.1684 (4)	−0.2255 (9)	3.37
C(64)	0.1534 (8)	0.2067 (4)	−0.3045 (10)	4.78
C(65)	0.0951 (7)	0.2209 (4)	−0.2141 (10)	4.64
B(1)	0.4815 (7)	0.1447 (4)	0.1040 (11)	3.20
B(2)	0.2409 (7)	−0.0332 (4)	0.1907 (11)	3.23
B(3)	0.0907 (7)	0.1909 (5)	0.0590 (12)	3.84
H(20)[a]	0.414	0.168	0.090	3.9
H(22)[a]	0.305	−0.007	0.179	3.9
H(24)[a]	0.100	0.141	0.072	3.9

[a] Positions of these H atoms were determined from a difference Fourier map and were not refined.

The ^1H NMR spectra of **1** and **2** are not useful in distinguishing these two possible interpretations because the BH_2 resonance is very broad due to quadrupolar coupling and relaxation effects from the boron atom. This is typical for polypyrazolylborate complexes.[1,2] To solve this problem, we prepared an isotopomer of **1**, $[D(\mu\text{-}D)B(pz)_2]_3Y$ (**1-d_6**). The deuterium resonance(s) of the BD_2 group in **1-d_6** should be considerably less broad than the hydrogen signal in **1**. Substitution of deuterium for hydrogen will lower boron coupling in the ^2H spectrum of **1-d_6** vs the ^1H spectrum of **1** by a factor of 6.5, the quotient of the H/D magnetogyric ratios. This lowering of J also has the effect of increasing the probability of ^{11}B becoming self-decoupled ($T_B^{-1} > J_{BD}$) from deuterium.[16] The ^2H NMR spectrum of **1-d_6** is a single line with a half-height width of 14 Hz. Thus, the deuterium atoms are equivalent at ambient temperature, and these data are consistent with the observation of a triplet in the ^{11}B spectrum.

We have investigated the ^{89}Y NMR spectrum of **1** in an attempt to observe proton coupling from a bridging B–H···Y interaction.

(16) Haris, R. K. *Nuclear Magnetic Resonance Spectroscopy*; Pitman: London, 1983; Chapter 5.

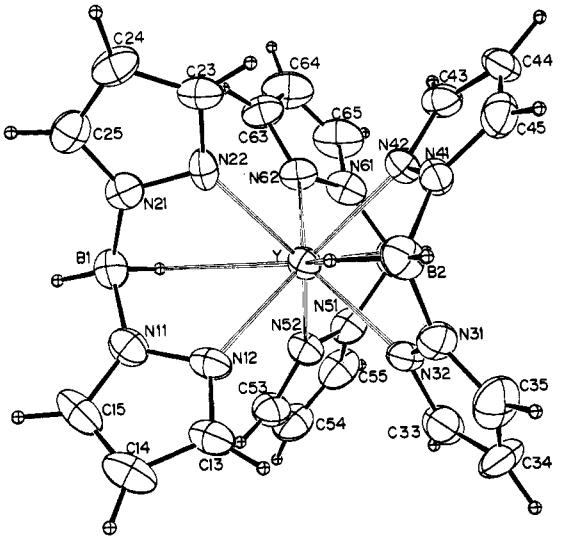

Figure 1. ORTEP drawing of $[H(\mu\text{-}H)B(pz)_2]_3Y$ as viewed from the center of a rectangular face (formed by N(12), N(22), N(32), N(42)) of the trigonal-prismatic arrangement of the six nitrogen donor atoms. Each of the rectangular faces is capped by a bridging B–H. The $B(3)H_2$ atoms are obscured by the $B(2)H_2$ atoms.

Even though the ^{89}Y nucleus is 100% abundant with spin = $^1/_2$, only a limited number of ^{89}Y NMR data are available. The early work in this area showed that ^{89}Y has a long relaxation time, necessitating the use of long pulse delays.[17] Evans and Closs[18] have recently published data on nine Cp–yttrium complexes that exhibit a chemical shift range of almost 400 ppm. Most relevant to our work, they report a Y–H coupling constant of 27 Hz for the bridging hydrogen atom in $[(MeC_5H_4)_2Y(\mu\text{-}H)(THF)]_2$. For **1**, the proton-coupled ^{89}Y spectrum shows a single resonance at 239.1 ppm with a half-height line width of 6.7 Hz. Although coupling could not be resolved, this resonance is broader than the 3.0-Hz half-height line width of the decoupled spectrum, indicating Y–H coupling. Also, the intensity of the resonance in the decoupled spectrum was diminished due to the negative NOE. The coupled ^{89}Y spectrum of **2** shows a single resonance at 105.6 ppm.

The above data were obtained in the normal, direct-detection pulsing mode. Reasonable signal to noise ratios could be obtained in ca. 4 h by using concentrated samples (ca. 0.3 M) in 10-mm NMR tubes. In order to obtain data with a very good signal to noise ratio for line-narrowing techniques, we used the INEPT[12] pulsing sequence to acquire ^{89}Y spectra of **1**. The advantage of this method is that the repetition time of the pulsing sequence is based on the fast relaxation time of ^1H rather than that of ^{89}Y, and a sensitivity gain of up to γ_H/γ_Y (a factor of 20) can be realized. This technique has been applied to hydrides of ^{187}Os[19] and ^{57}Fe[20] and a series of (diene)M (M = W, Mo) complexes.[21] Using this method, we were able to acquire high-quality spectra in 6 min. Although even with line-narrowing techniques it did not prove possible to resolve J_{YH} in the coupled spectrum, the very fact that the method was successful proves that coupling exists. The value of J_{YH} was determined to be 0.5 Hz by measuring the intensity of the signal vs the polarization transfer delay in the refocussed INEPT sequence. The most effective transfer of magnetization occurs with a delay of $1/4J$.

Table III. Interatomic Distances (Å) and Angles (deg) Relevant to Yttrium Coordination Sphere (Esd's in Parentheses)

Bond Distances			
Y(1)–N(12)	2.392 (6)	Y(1)–N(42)	2.378 (6)
Y(1)–N(22)	2.396 (5)	Y(1)–N(52)	2.395 (7)
Y(1)–N(32)	2.389 (6)	Y(1)–N(62)	2.387 (7)
Bond Angles			
N(12)–Y(1)–N(22)	81.1 (2)	N(22)–Y(1)–N(62)	81.2 (2)
N(12)–Y(1)–N(32)	81.5 (2)	N(32)–Y(1)–N(42)	79.7 (2)
N(12)–Y(1)–N(42)	136.1 (2)	N(32)–Y(1)–N(52)	84.3 (2)
N(12)–Y(1)–N(52)	83.2 (2)	N(32)–Y(1)–N(62)	137.4 (2)
N(12)–Y(1)–N(62)	135.3 (2)	N(42)–Y(1)–N(52)	133.3 (2)
N(22)–Y(1)–N(32)	133.9 (2)	N(42)–Y(1)–N(62)	81.9 (2)
N(22)–Y(1)–N(42)	84.0 (2)	N(52)–Y(1)–N(62)	81.0 (2)
N(22)–Y(1)–N(52)	135.0 (2)		

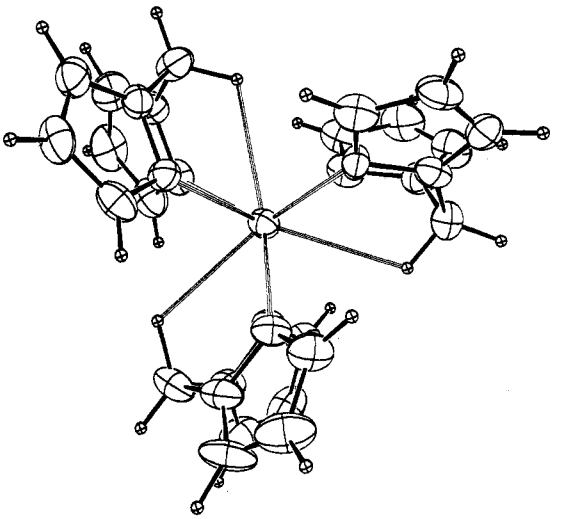

Figure 2. ORTEP drawing of $[H(\mu\text{-}H)B(pz)_2]_3Y$ as viewed down one of the triangular faces of the trigonal prism formed by the six nitrogen donor atoms.

The ^1H and ^{13}C NMR spectra of **1** show only three resonances in the aromatic region. Thus, the pyrazolyl rings either are equivalent in the solution structure or are undergoing a dynamic rearrangement. An interesting feature of the carbon spectrum is the observation of Y–C coupling ranging from 0.5 to 1.5 Hz in each of the three carbon resonances. The ^{13}C MAS solid-state spectrum also shows only these three resonances. The dimethyl-substituted complex, **2**, shows equivalent pyrazolyl rings in solution ^1H and ^{13}C ambient-temperature NMR spectra.

Molecular Structure of $[H(\mu\text{-}H)B(pz)_2]_3Y$. The solid-state structure of **1** has been determined. The geometry of the six nitrogen donor atoms of **1** is a trigonal prism. Figure 1 shows an ORTEP drawing of the molecule as viewed from the center of one of the rectangular faces. Figure 2 shows a second view projecting down one of the triangular faces of the trigonal prism. The $CDCl_3$ of crystallization is disordered and not shown. The two triangular faces of the trigonal prism (formed by N(12), N(32), N(52) and N(22), N(42), N(62)) are parallel and are at right angles to the rectangular face N(12), N(22), N(32), N(42) (the deviations from the least-squares plane of these four atoms are less than 0.023 Å). The yttrium atom is 0.028 Å out of the plane formed by the three boron atoms, and this plane is parallel to the two triangular planes of nitrogen atoms. Thus, while not crystallographically imposed, there is a near-mirror plane containing the yttrium and the three boron atoms. The twist angle between the two N_3 faces is nearly 0°, as expected for a trigonal prism.

The outstanding structural feature of this molecule is that each of the three rectangular faces of the trigonal prism are capped by a bridging B–H···Y three-center bond. This interaction is most clearly defined by the short Y–B distances, which average at 3.211 Å, and the location of the bridging hydrogen atoms close to yttrium in the difference Fourier map. For cases where no three-center

(17) (a) Levy, G. C.; Rinaldi, P. L.; Bailey, J. T. *J. Magn. Reson.* **1980**, *40*, 167. (b) Adam, R. M.; Fazakerly, G. V.; Reid, D. G. *J. Magn. Reson.* **1979**, *33*, 655. (c) Kronenbitter, J.; Schwenk, A. *J. Magn. Reson.* **1977**, *25*, 147. (d) Habler, C.; Kronenbitter, J.; Schwenk, A. *Z. Phys. A* **1977**, *280*, 117.
(18) Evans, W. J.; Meadows, J. H.; Kostka, A. G.; Closs, G. L. *Organometallics* **1985**, *4*, 324.
(19) Cabeza, J. A.; Mann, B.; Brevard, Ch.; Maitles, P. M. *J. Chem. Soc., Chem. Commun.* **1985**, 65.
(20) Benn, R.; Brevard, Ch. *J. Am. Chem. Soc.* **1986**, *108*, 5622.
(21) Benn, R.; Brevard, Ch.; Rufinska, A.; Schroth, G. *Organometallics* **1987**, *6*, 938.

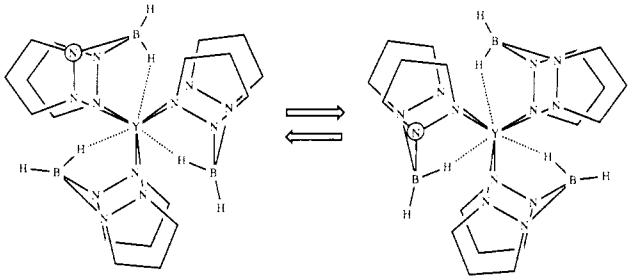

Figure 3. Drawing of a possible rearrangement for the equilibration of the BH_2 hydrogen atoms in a capped trigonal-prismatic geometry. The agostic B–H···Y bonds break, the six-membered BN_4Y rings flip from one boat configuration to the other, and the B–H···Y bonds re-form on the adjacent rectangular faces of the trigonal prism. A nitrogen atom of the top pyrazolyl ring for one ligand is circled for emphasis.

interaction exists for this ligand, the puckering of the six-member chelate ring is shallow with M–B distances of ca. 3.8 Å.[22] While the B–Y distance for **1** is 0.25–0.31 Å longer than the comparable distances in **3** and **4**, when corrected for the difference in size of these metals,[23] it is only 0.07–0.12 Å longer. This again indicates that the three-center interactions are weaker in **1** than in the other previously prepared examples but unequivocally demonstrates that a B–H···Y interaction exists in the solid state.

Multinuclear Variable-Temperature NMR Investigations. The solid-state structure of **1** and the IR spectra in both the solid and solution phases clearly indicate three-center B–H···Y interactions that render the BH_2 hydrogen atoms nonequivalent. However, in the ambient-temperature ^{11}B and ^{2}H NMR spectra they appear as equivalent, indicating an equilibration by a dynamic process. The most obvious mechanism for such an equilibrium involves breaking the three-center interactions, flipping the boat-shaped six-membered YN_4B rings (this ring flipping has been shown to have a barrier of ca. 6 kcal/mol),[24] and re-forming the three-center interactions on the other adjacent rectangular face of each ligand (Figure 3). This type of dynamic rearrangement has not been observed for the other examples of molecules showing a three-center interaction with this ligand, even at elevated temperatures. For example, the ^{11}B spectrum of **3** described above remains as a doublet of doublets at 110 °C.[1b] In contrast, this type of ring flip has been proposed to explain the high-temperature dynamic behavior of $[Et(CH_3CH(\mu\text{-}H))B(pz)_2]Mo(CO)_2(\eta^3\text{-allyl})$ complexes.[24] These molecules have a C–H···Mo three-center interaction involving the methylene hydrogen atoms. The activation energy for the process is 17–20 kcal/mol. The observation of the ring flip in these cases, but not with $[H(\mu\text{-}H)B(3,5\text{-}Me_2pz)_2]Mo(CO)_2(\eta^3\text{-}C_7H_7)$, was explained by a stronger three-center interaction in the latter case due to the fact that the B–H bond would be more polarized toward the hydrogen atom than a C–H bond and, thus, be able to form a stronger interaction with the metal.

Note that if the trigonal-prismatic structure found in the solid state of **1** is retained in solution, the dynamic process shown in Figure 3 should not affect the pyrazolyl ring hydrogen and carbon atom resonances because these rings are equivalent in this highly symmetrical structure. Nevertheless, all three carbon resonances in the ^{13}C spectrum broaden below −29 °C, sharpening at lower temperatures until at −83 °C two equal-height resonances are observed for each resonance type (Figure 4). In the ^{1}H spectra, at lower temperatures only one of the pyrazolyl ring hydrogen atom resonances noticeably broadens at ca. −29 °C, sharpening to a single resonance at −64 °C. The barrier to the dynamic process that is responsible for these observations is 11.4 kcal/mol at −53 °C, as calculated from the carbon data. Complex **2** shows similar fluxional behavior with a measured barrier to equilibration of 11.8 kcal/mol.

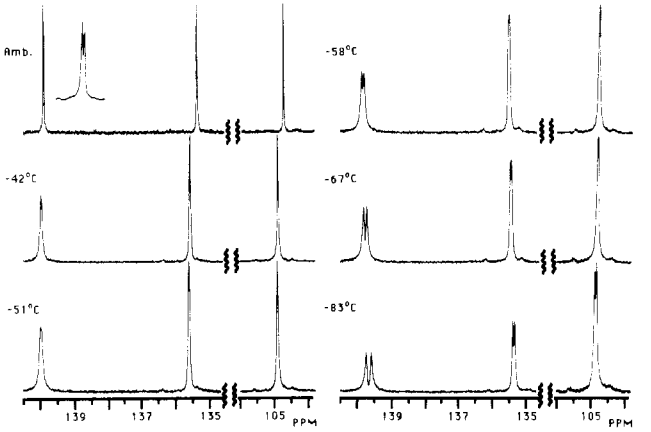

Figure 4. Variable-temperature ^{13}C NMR spectra for $[H(\mu\text{-}H)B(pz)_2]_3Y$. The expansion in the ambient-temperature spectrum shows C–Y coupling to the 139.7 ppm resonance.

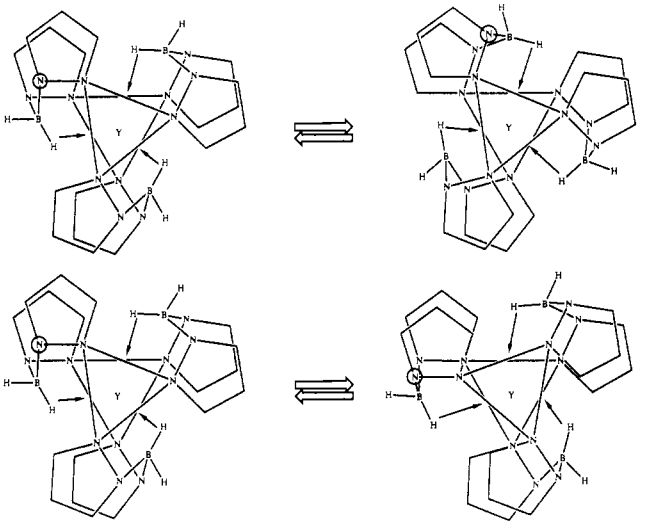

Figure 5. Top: Rearrangement of the C_3 solution structure by breaking the B–H···Y bonds, flipping the BN_4Y rings, and re-forming the agostic interaction on the adjacent face. This process, similar to that shown in Figure 3 for a trigonal-prismatic structure, equilibrates the pyrazolyl rings and the BH_2 hydrogen atoms. Bottom: Rearrangement of the C_3 solution structure by counterclockwise rotation of the top triangular face relative to the bottom. This process equilibrates the pyrazolyl rings, but not the BH_2 hydrogen atoms. A nitrogen atom of the top pyrazolyl ring for one ligand is circled in each structure for emphasis.

This observation of two equally intense resonances for each pyrazolyl ring carbon atom type can be explained by a solution structure that differs from the solid-state structure by rotation of one 3-fold N_3 face relative to the other. Figure 5 shows examples of an arrangement of the donor nitrogen atoms of this type. An octahedral arrangement of the nitrogen donor atoms is the limiting structure (C_3 symmetry). In any rotated structure the top and bottom pyrazolyl rings are nonequivalent (only one donor atom of each ligand is part of a triangular face that is capped by an adjacent ligand).

It is not clear why the solution structure is different from the solid-state structure. These spectra were all run in the polar solvent CD_2Cl_2, but similar variable-temperature spectra are observed in the less polar solvent toluene-d_6. Kepert[25] has argued that the ratio of the bite of the chelate ring to the metal–donor distance, b, can be used to explain the structures of tris(bidentate ligand) complexes. From the solid-state structure, our calculated b value (N–N intraligand distance/N–Y distance) is low at 1.29. Small bites favor distortion of the octahedron toward the trigonal prism. On the basis of the curve presented in ref 25, the twist angle of the two triangular faces would be predicted to be ca. 48° (an

(22) Cotton, F. A.; Frenz, B. A.; Murillo, C. A. *J. Am. Chem. Soc.* **1975**, *97*, 2118.
(23) *Handbook of Chemistry and Physics*; Weast, R. C., Ed.; CRC: Cleveland, OH, 1965; p F117.
(24) Cotton, F. A.; Stanislowski, A. G. *J. Am. Chem. Soc.* **1974**, *96*, 5074.
(25) Kepert, D. L. *Inorg. Chem.* **1972**, *11*, 1561.

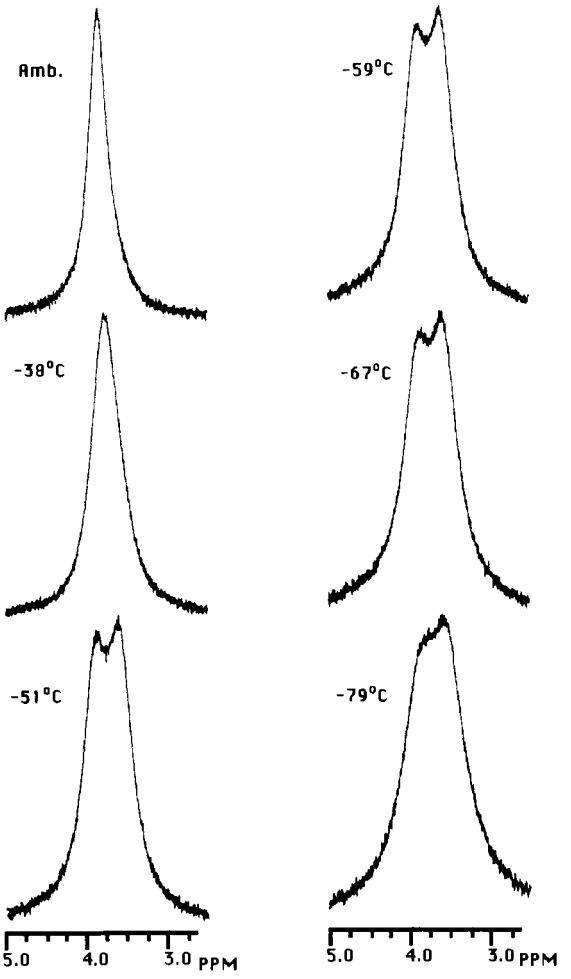

Figure 6. Variable-temperature ^2H NMR spectra for $[D(\mu\text{-}D)B(pz)_2]_3Y$.

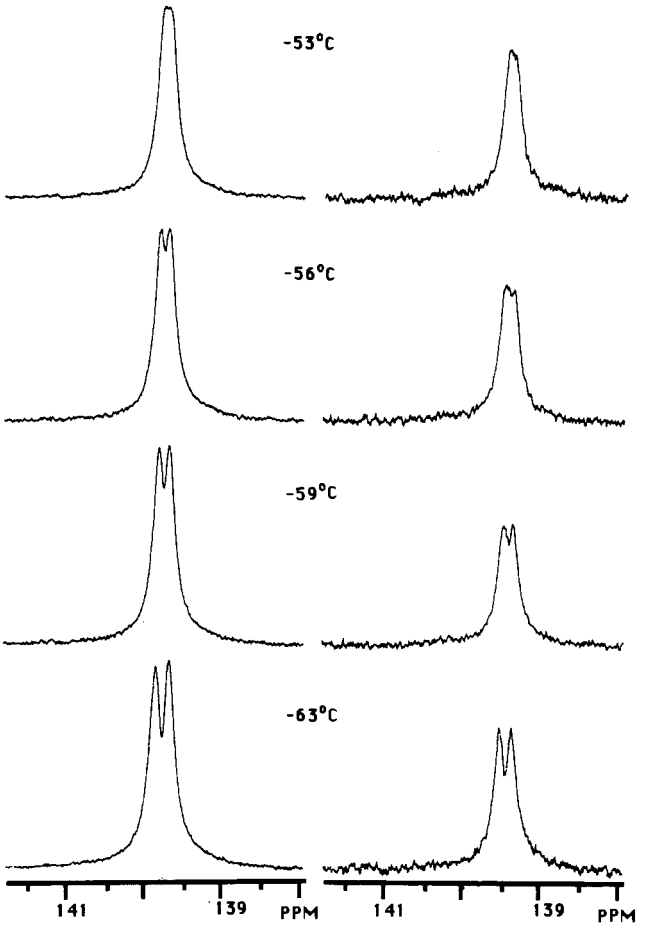

Figure 7. Variable-temperature ^{13}C NMR spectra for $[H(\mu\text{-}H)B(pz)_2]_3Y$ (left) and $[D(\mu\text{-}D)B(pz)_2]_3Y$ (right) for the most deshielded resonances near the coalescence temperatures.

octahedron has a twist angle of 60°). These arguments may not directly apply to **1** because it is formally nine-coordinate, but indicate that the trigonal prism is a reasonable structure. What is clear from our data is that crystal-packing forces favor the trigonal-prism structure whereas solvation forces favor the rotated structure.

In the variable-temperature ^1H NMR spectra, the BH_2 resonance stays very broad until ca. −48 °C. Below this temperature, it resolves into two broad resonances separated by 0.34 ppm. Two effects are needed to explain these data. First, lowering the temperature (and increasing the solvent viscosity) decreases the boron relaxation time such that it becomes self-decoupled from the hydrogen atoms.[16] Second, the appearance of two resonances indicates that these two hydrogen atoms are nonequivalent, as expected from the X-ray structure and IR data. What cannot be determined from these data is the multiplicity of the very broad ambient-temperature resonance. At the temperatures that the boron self-decoupling becomes efficient, two resonances are already observed. The observation of a triplet in the ambient-temperature ^{11}B data indicates that these hydrogen atoms should be equivalent in the ^1H spectrum at this temperature, but the point cannot be definitively proven. While meaningful ^1H data can only be obtained at low temperature, low-temperature ^{11}B data were not useful because the signal becomes extremely broad below −40 °C due to the fast relaxation of boron at these temperatures. Thus, from the ^{11}B data the hydrogen atoms appear to be equivalent at ambient temperature and from the ^1H data they appear to be nonequivalent at low temperature, but experimental limitations prevent either from showing both types of behavior. Variable-temperature ^{89}Y NMR spectroscopy also did not solve this problem because J_{YH} could not be resolved at any temperature.

It did prove possible to observe ^2H NMR spectra in both temperature ranges for **1**-d_6 (Figure 6). A single resonance is observed at ambient temperature that broadens at lower temperatures, resolving into two equal-intensity resonances at −51 °C. Deuterium, like boron, is quadrupolar, but the resonances remain fairly sharp, and although broadened somewhat, the two resonances are still clearly resolvable at −67 °C. These deuterium data indicate that the two resonances observed at low temperature in the ^1H spectra for the BH_2 group arise from a bridging and nonbridging hydrogen atom. The coalescence of these lines can be used to set a lower limit of 11 kcal/mol for the process that equilibrates the two hydrogen atoms. This is only a lower limit because coupling and quadrupolar broadening contribute to the line shape.

Thus, the barrier to the dynamic process that equilibrates the pyrazolyl ring carbon atoms is about the same as that to the process that equilibrates the hydrogen atoms of the BH_2 groups. The mechanism for the equilibration of the BH_2 protons shown in Figure 3 but applied to the correct solution structure of C_3 symmetry is shown in the top of Figure 5. This process would also equilibrate the pyrazolyl rings and, thus, could also explain the carbon data. Another reasonable mechanism to equilibrate the pyrazolyl rings is rotation of one triangular face with respect to the other through the trigonal-prismatic solid-state structure, as shown in the bottom of Figure 5. This mechanism equilibrates the rings without equilibrating the BH_2 hydrogen atoms. Breaking of the agostic interactions is needed for this equilibration. The similarity of the barriers for the two types of fluxional processes does indicate that the mechanisms for both are the same, but it is by no means proof.

In order to obtain more definitive information on this point, we have carefully measured the coalescence temperatures for equilibration of the carbon atoms of **1** and **1**-d_6. Because of the greater zero-point energy of a B–H vs a B–D group, the strengths of the agostic B–H···Y and B–D···Y interactions should be different. This type of energy difference has been used to prove agostic interactions by comparing the ^1H chemical shift values

of CH_3 vs CH_2D groups.[26] For **1** and **1-d_6**, the difference in zero-point energies should lead to a different barrier to ring equilibration if the bond-breaking mechanism shown in the top of Figure 5 is correct, but the barrier would be the same for the rotational motion shown in the bottom of Figure 5.

Figure 7 shows the ^{13}C NMR spectra of the most deshielded resonance of **1** and **1-d_6** in the temperature range of their coalescence. In the limiting low-temperature spectrum (-83 °C), the separation of the resonances for both complexes is the same (11.3 Hz) and both have the same half-height width. Thus, no isotope effects or C-D coupling is observed in these resonances for **1-d_6**. At -59 °C, the resonances are collapsing such that the separation is 5.1 Hz for **1** and 4.4 Hz for **1-d_6**. At -56 °C, **1-d_6** is at its coalescence temperature whereas a separation of 4.3 Hz is still observed for **1**. Coalescence is reached for **1** at -53 °C. The calculated energy difference for the two molecules is only 0.2 kcal/mol, but the spectra clearly indicate a difference. While not large, this difference strongly indicates that the process that equilibrates the pyrazolyl rings involves bond breaking of the B-H···Y interaction. Thus, both of the fluxional processes observed for **1** are believed to be caused by the molecular motion shown in the top of Figure 5.

Conclusions

The complexes $[H(\mu\text{-}H)B(pz)_2]_3Y$ (**1**) and $[H(\mu\text{-}H)B(3,5\text{-}Me_2pz)_2]_3Y$ (**2**) are readily prepared from YCl_3 and the ligand salt. The solid-state structure of **1** has been determined crystallographically. It consists of a trigonal-prismatic arrangement of the nitrogen donor atoms with each of the three rectangular faces capped by a bridging, three-center B-H···Y interaction. The bridging interaction is confirmed in both the solid and solution phases for **1** and **2** by the observation of low B-H stretching bands in the IR and in solution by the nonequivalence of the BH_2 resonances in low-temperature NMR spectra. The pyrazolyl rings of both complexes also show as a 1/1 nonequivalent set in low-temperature ^{13}C NMR spectra. The molecules show dynamic rearrangements in solution with both the BH_2 proton and pyrazolyl carbon signals collapsing to a single set of resonances above 0 °C. This observation for the BH_2 group was confirmed from ^2H NMR data on $[D(\mu\text{-}D)B(pz)_2]_3Y$ (**1-d_6**). As the pyrazolyl rings are equivalent in the solid-state structure, we propose in solution that the triangular faces of the trigonal prism are rotated toward an octahedral type arrangement. The dynamic processes that equilibrate the BH_2 and pyrazolyl rings have very similar barriers and are believed to arise from a single molecular rearrangement. The mechanism proposed involves breaking the three-center interactions, flipping the boat-shaped YN_4B rings, and re-forming the three-center interactions on the other adjacent faces. This mechanism is supported by the measurement of a slightly different barrier to equilibration of the pyrazolyl rings in **1** vs that in **1-d_6**.

Acknowledgment. We wish to thank Dr. Paul Ellis for running the solid-state ^{13}C NMR spectra and for useful discussions. We thank Dr. Ron Garber for assistance with the ^{89}Y NMR data and Dr. Richard D. Adams and Dr. Jack Faller (Yale University) for discussions of the variable-temperature NMR data. The NSF (Grant CHE-8411172) and NIH (Grant RR-02425) have supplied funds to support NMR equipment, and the NIH (Grant RR-02849) has supplied funds to support mass spectrometry equipment.

Registry No. **1**·$CHCl_3$, 114094-42-7; **2**, 114094-43-8; **1-d_6**, 114094-44-9; Y, 7440-65-5.

Supplementary Material Available: Table IV (bond distances and angles for the ligands), Table V (positional parameters of H atoms), and a table listing anisotropic thermal parameters (6 pages); a table of structure factor amplitudes (14 pages). Ordering information is given on any current masthead page.

(26) (a) Calvert, R. B.; Shapley, J. R. *J. Am. Chem. Soc.* **1978**, *100*, 7726. (b) Casey, C. P.; Fagan, P. J.; Miles, W. H. *J. Am. Chem. Soc.* **1982**, *104*, 1134.

Contribution from the Department of Chemistry, State University of New York at Albany, Albany, New York 12222

Synthesis and Structural Characterization of a Tetramolybdate, $[Mo_4O_{12}(C_8H_6N_4)]^{2-}$, Containing a Bridging Phthalazine-1-hydrazido(2-) Ligand. Comparison to the Structure of $[Mo_4O_{10}(OMe)_2(NNMePh)_2]^{2-}$, a Tetramolybdate Species Exhibiting Ligation to a Terminal Monodentate Hydrazido(2-) Group

Shahid N. Shaikh and Jon Zubieta*

Received October 23, 1987

The reaction of $(n\text{-}Bu_4N)_2[Mo_2O_7]$ with 1-methyl-1-phenylhydrazine in CH_2Cl_2-methanol yields the tetranuclear poly oxomolybdate $(n\text{-}Bu_4N)_2[Mo_4O_{10}(OCH_3)_2(NNMePh)_2]$ (I). Complex I displays the methoxy-bridged binuclear core $[MoO(NNMePh)(\mu\text{-}OCH_3)_2MoO(NNMePh)]^{2+}$, bridged by two double-bridging bidentate $[MoO_4]^{2-}$ units. Complex I is structurally related to the class of tetranuclear poly oxomolybdates coordinated to small organic molecules, $[Mo_4O_{6-10}L_1L_2]^{n-}$. The reaction of $(n\text{-}Bu_4N)_2[Mo_2O_7]$ with the potentially chelating and bridging hydrazino ligand hydrazinophthalazine, $H_2NNH(C_8H_5N_2)$ (H_2NNH-pht), yields the analogous tetranuclear species $(n\text{-}Bu_4N)_2[Mo_4O_{12}(HNN\text{-}pht)]$ (II). Although structurally related to I, II reveals a number of distinctive features. The binuclear core $[Mo_2O_4(HNN\text{-}pht)]^{2+}$ displays a bridging oxo group and a bidentate bridging phthalazine moiety, in contrast to the two bridging methoxy groups of I. The Mo centers of this core are nonequivalent, one exhibiting $[MoO_4N_2]$ coordination and the other $[MoO_5N]$. The bridging $[MoO_4]^{2-}$ moieties display unexceptional geometry. The ^{17}O NMR spectra of I, II, and the related 1,4-dihydrazinophthalazine derivative $[Mo_4O_{11}(C_8H_6N_6)]^{2-}$ are consistent with the solid-state structures, exhibiting resonances in the regions assigned to doubly bridging Mo_2O groups (350-450 ppm) and to terminal MoO groups (750-950 ppm). Crystal data follow. For I: monoclinic space group $P2_1/c$, with a = 9.770 (2) Å, b = 18.633 (3) Å, c = 16.706 (3) Å, β = 90.74 (1)°, V = 3041.0 (12) Å, Z = 2, and D_{calcd} = 1.45 g cm^{-3}; structure solution based on 1571 reflections converged at R = 0.0647. For II: triclinic space group $P\bar{1}$, with a = 16.528 (2) Å, b = 17.631 (3) Å, c = 19.539 (4) Å, α = 88.90 (1)°, β = 87.00 (1)°, γ = 88.10 (1)°, V = 5682.2 (24) Å^3, Z = 4, and D_{calcd} = 1.43 g cm^{-3}; structure solution based on 5429 reflections converged at 0.0689.

The coordination compounds of isopoly oxomolybdates continue to attract considerable attention as models for the interactions of small organic molecules with catalytic oxide surfaces.[1,2] The coordination chemistry of the isopoly oxomolybdate anions with

0020-1669/88/1327-1896$01.50/0